

# Decentralized Demand Response for Energy Hubs in Integrated Electricity and Gas Systems Considering Linepack Flexibility

Sheng Wang, *Member, IEEE*, Hongxun Hui, *Member, IEEE*, Yi Ding, *Member, IEEE*, and Junyi Zhai, *Member, IEEE*

**Abstract**—The wide application of energy conversion facilities on the demand side (e.g., combined heat and power units) has accelerated the integration of multiple energies in the form of Energy Hub (EH). EH can schedule its electricity and gas consumption patterns flexibly to provide demand response (DR) services to the electricity system. However, the DR can lead to high uncertainties of gas demands, threatening the real-time balance of the integrated electricity and gas systems (IEGS). The gas stored in the pipeline (i.e., linepack) is a promising flexible resource to accommodate the gas demand uncertainties during the DR. However, the linepack is governed by the complex physical characteristics of gas flow dynamics, which is challenging to use. This paper proposes a coordinated optimal control framework for both EH and IEGS, focusing on utilizing the linepack flexibility to promote the DR capability. First, we develop a multi-level self-scheduling framework for the EH to comprehensively explore the DR potential. The constraints of gas flow dynamics are then formulated to ensure that the fluctuated gas demand can be accommodated by the linepack in the IEGS. The second-order-cone (SOC) relaxation is adopted to convexify the nonlinearity in the motion equation of gas flow dynamics. Moreover, to tackle the overall mixed-integer SOC programming problem, we propose an enhanced Benders decomposition strategy by embedding the lift-and-project cutting plane method, and further devise a novel solution procedure. Finally, the IEEE 24-bus Reliability Test System and the Belgium natural gas transmission system are used to validate the effectiveness of the proposed method.

**Index Terms**—energy hub, integrated electricity and gas systems, demand response, self-schedule, gas flow dynamics.

## I. INTRODUCTION

WITH the rising concern for low-carbon development, the coordinated utilization of different energies (e.g., electricity, gas, and heat) has become one of the most appealing ways to promote energy efficiency [1]. On the demand side, different energies are linked through local devices, such as combined heat and power plants (CHP), electric heat pumps (EHP), etc. They consume energies from both electricity and gas systems to satisfy the electricity, heating, and cooling demands of end-users [2]. Under this background, the concept of energy hub (EH) is developed to feature the energy conversion process from multiple energy supplies to multiple

(Corresponding author: Hongxun Hui)

Sheng Wang is with the State Key Laboratory of Internet of Things for Smart City, the Department of Electrical and Computer Engineering, University of Macau, Macao, 999078, China (email: [wangsheng\\_zju@zju.edu.cn](mailto:wangsheng_zju@zju.edu.cn)).

Hongxun Hui is with the State Key Laboratory of Internet of Things for Smart City and the Department of Electrical and Computer Engineering, University of Macau, Macao, 999078, China (email: [hongxunhui@um.edu.mo](mailto:hongxunhui@um.edu.mo)).

Yi Ding is with the College of Electrical Engineering, Zhejiang University, Hangzhou, 310058, China (email: [yiding@zju.edu.cn](mailto:yiding@zju.edu.cn)).

Junyi Zhai is with the College of New Energy, China University of Petroleum (East China), Qingdao, 266580, China (email: [zhaijunyi@upc.edu.cn](mailto:zhaijunyi@upc.edu.cn)).

energy consumptions [3].

The EH not only integrates multiple energies, but also diversifies the path to meet energy demands [4]. For example, the heating demand supplied by the EHP can be covered by ramping up the heat production of the CHP. By this means, the total electricity consumption can be reduced, while the gas consumption of the CHP increases. This trade-off among different energy consumptions in the EH is defined as energy substitution, which can be utilized to provide demand response (DR) service to the electricity system [5, 6]. Some studies have been carried out on this kind of DR. For example, energy substitution is used to flexibly supply the electrical, heating, and cooling demands for a building in [7]. The EH scheduling problem is developed as a mixed-integer nonlinear programming (MINLP) based on a probabilistic model in [8]. Apart from theoretical research, practical projects have also witnessed the potential of energy substitution in EH (e.g., the test-bed plant in Spain [9]). Compared with traditional DR in electricity systems only (e.g., changing the charging/discharging patterns of electric vehicles [10], switching off air conditioners [11], etc.), the energy substitution in EH has less interruption to users' demands [12]. However, there are *three main challenges* of providing DR in EHs:

- 1) *Multi-strategy cooperation*: Apart from the energy substitution, there are other flexible DR strategies in EH. Temporal load shifting and initiative load curtailment are also effective in reducing the peak load and flattening the load curve in the traditional electricity system [13]. Some studies have tentatively incorporated the temporal load shifting and initiative load curtailment strategies into the DR in EHs. For example, the flexible energy load in EHs is divided into primary load and deferable load in [14], but the deferable load does not need to be recovered mandatorily. The load shifting process in [15] only forces the balance of shift-out and shift-in loads within a long period, while the real-time balance and time-interdependency in the load shifting are not considered.

In summary, the temporal load-shifting models in previous studies are relatively rough, which cannot reflect the time-interdependency of the load-shifting process [16]. Moreover, the DR potential has not been fully excavated by cooperatively using these three strategies. However, introducing the time-dependent temporal load shifting will increase the computation complexity of the original EH scheduling problem. Therefore, efficient modeling and solution methodologies are urgently needed.

- 2) *Multi-system coordination*: Generally, there are multiple EHs on the demand side, which consume both electricity and

> REPLACE THIS LINE WITH YOUR MANUSCRIPT ID NUMBER (DOUBLE-CLICK HERE TO EDIT) <

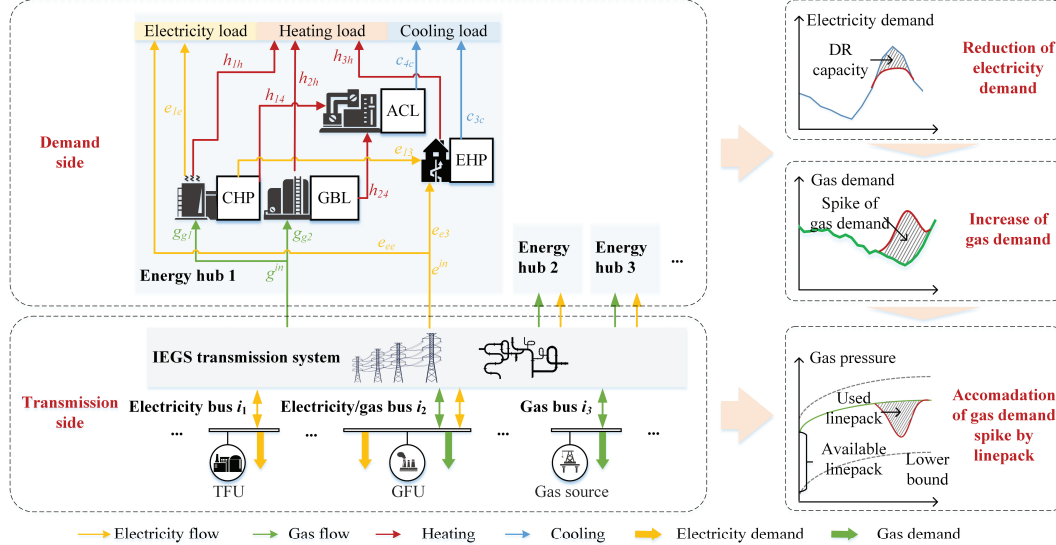


**Fig. 1.** Coordination framework of the IEGS and EHs for providing DR by using linepack.

gas from the integrated electricity-gas systems (IEGS). During the DR, the energy substitution of the EH may lead to a spike in gas demand, which further endangers the IEGS operation [17]. The gas stored in the pipeline (i.e., linepack) is a flexible and accessible resource across the gas network [18]. It can be utilized to accommodate the gas demand spikes at various locations, if the EHs and IEGS are well coordinated.

In previous studies, the coordination of EHs and IEGS is usually investigated using the steady-state gas flow model [19, 20]. However, considering the time scale of DR is close to real-time, the modeling of linepack should obey the physical laws that govern the gas flow dynamics [21]. Therefore, incorporating the time-dependency of gas flow dynamics is challenging, especially when it is also coupled with the time-dependency of EH scheduling. Some studies have investigated the linepack utilization for optimal dispatch [22] and resilience management [23], etc., but its application in DR and the coordination with EHs remains unexplored.

3) *Computation viability:* The comprehensive optimization of IEGS and EHs is a large-scale, time-dependent, and nonlinear optimal control problem, especially after incorporating various DR strategies and gas flow dynamics. These characteristics may make the traditional centralized solution methods less efficient or robust.

In previous research, because their coordination problems are usually time-independent and the scale of the problem is relatively small, the centralized solution methods are still adequate. For example, some of the studies retain the nonlinear forms of the optimization problem, and solve it using the IPOPT solver [19] or heuristic algorithm [24]. Some studies convexify the problem by linearizing the quadric term of the gas flow equations around the normal operating point [25]. The piecewise linearization and second-order cone relaxation techniques are also used in [26] and [27], respectively. However, these solution methods cannot be directly applied to our large-scale and time-dependent DR problem, and a new solution strategy is needed.

To address the above research gaps, this paper proposes a decentralized DR framework for IEGS and EHs. The contributions are summarized as follows:

1) A multi-level self-scheduling model for the EH is proposed to excavate DR potential. Compared with previous studies, the proposed model can cooperate the energy substitution, load shifting, and initiative load curtailment strategies. By using the McCormick envelope, the time interdependency in the load shifting can be characterized more precisely and tractably.

2) A coordinated optimal control framework of the IEGS and EHs is proposed for providing DR service. Compared with the traditional steady-state-based framework, the proposed framework can utilize linepack flexibilities to accommodate the gas demand spikes during the DR. The second-order-cone (SOC) reformulation is tailored to convexify the gas flow dynamic equations, so that it can be addressed by off-the-shelf solvers.

3) An enhanced Benders decomposition (EBD) is developed to solve the coordinated optimal control problem in a decentralized manner to protect privacy. The Lift-and-project (L&P) cutting plane method is embedded to tackle the integer variables in the subproblems. Moreover, a novel solution procedure is designed, which utilizes the multi-level structure of the EH self-scheduling problem to promote computation efficiency.

## II. STRUCTURE OF THE IEGS AND EHs

The structure of the IEGS and EHs is presented in Fig. 1. On the transmission side, the IEGS transports the electricity and gas from generating units (i.e., gas-fired generating units and traditional fossil units) and gas sources (i.e., gas wells and storages) to the demand side, respectively. The gas-fired generating unit (GFU) consumes gas to generate electricity, which is the key linkage between the two energy systems (i.e., gas and electricity systems). On the demand side, districts such as the campus, industrial park, and buildings, can be modeled

> REPLACE THIS LINE WITH YOUR MANUSCRIPT ID NUMBER (DOUBLE-CLICK HERE TO EDIT) <

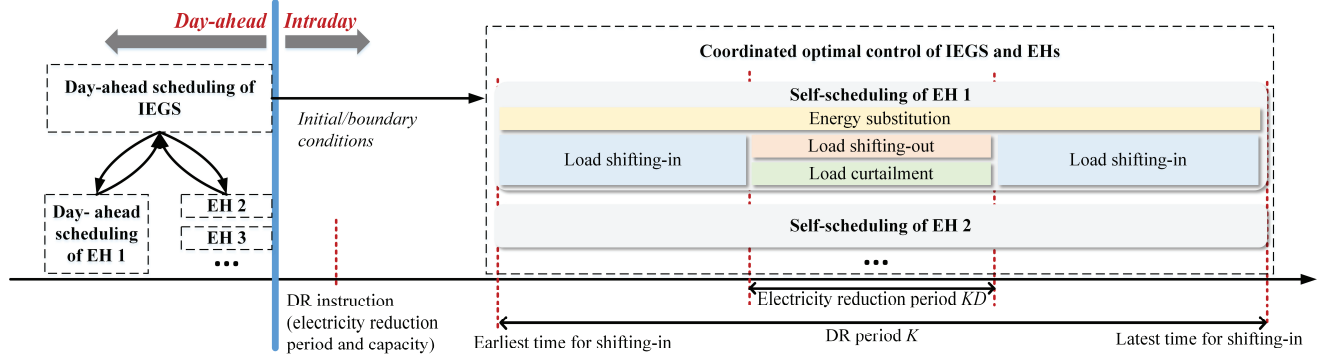


Fig. 2. Implementation timeline of DR in the IEGS and EHs.

as EHs [28]. In this paper, we consider a typical configuration of the EH, including the CHP, gas boiler (GBL), EHP, and absorption chiller (ACL).

Fig. 1 and Fig. 2 jointly show the implementation process of DR. During the operation, the DR instruction (including electricity reduction period and capacity) will be broadcast to each EH. Based on that, the EHs will implement multi-level self-scheduling to provide the required DR service for the given period. The self-scheduling strategies include energy substitution, load shifting, and load curtailment. They are implemented in different time periods, as shown in Fig. 2. The self-scheduling of EHs is effective in reducing the electricity demand, while the gas demand may increase dramatically. Then, the linepack in the gas pipeline can be used to accommodate the gas demand spike by lowering the gas pressure momentarily within the secure range. Therefore, considering the physical interaction of IEGS and EHs, a coordination framework is required for providing the DR service in a globally optimal way.

### III. MULTI-LEVEL SELF-SCHEDULING MODEL OF THE EH

The operating schedule of the EH is usually determined in the day-ahead to satisfy the forecasted electricity, heating, and cooling loads. The DR instruction can be broadcast to the EH either in the day-ahead or during intraday operation. Once the instruction is received, the EH will implement the self-scheduling strategy to adjust the operating condition and satisfy the DR requirement. Therefore, both day-ahead scheduling and intraday self-scheduling are studied in this section.

#### A. Optimal Scheduling of the EH in the Day-Ahead

The objective of the optimal scheduling in the day-ahead is to minimize the energy purchasing cost  $C_{EH}$  on an hourly basis:

$$\underset{e^{in}, g^{in}, \mathbf{x}^{st}}{\text{Min}} \quad C_{EH} = \rho^e \times e^{in} + \rho^g \times g^{in} \quad (1)$$

s.t.

$$\mathbf{H}_{11 \times 15} \begin{bmatrix} e^{in} & g^{in} & \mathbf{x}^{st} \end{bmatrix}^T = \begin{bmatrix} d^{el} & d^{ht} & d^{cl} & \mathbf{0}_{1 \times 8} \end{bmatrix}^T \quad (2)$$

$$h_{1h} + h_{14} \geq 0 \quad (3)$$

$$e_{13} + e_{le} - E_A - (E_A - E_B)/(H_A - H_B)(h_{1h} + h_{14}) \leq 0 \quad (4)$$

$$e_{13} + e_{le} - E_B - (E_B - E_C)/(H_B - H_C)(h_{1h} + h_{14} - H_B) \geq 0 \quad (5)$$

$$e_{13} + e_{le} - E_D - (E_C - E_D)/(H_C - H_D)(h_{1h} + h_{14}) \geq 0 \quad (6)$$

$$ho_2^- \leq h_{24} + h_{2h} \leq ho_2^+ \quad (7)$$

$$co_4^- \leq c_{4c} \leq co_4^+ \quad (8)$$

$$\gamma ho_3^- \leq h_{3h} \leq \gamma ho_3^+ \quad (9)$$

$$(1-\gamma)co_3^- \leq c_{3c} \leq (1-\gamma)co_3^+ \quad (10)$$

$$\mathbf{x}^{st} \geq 0 \quad (11)$$

where  $\mathbf{H}$  is the sparse energy conversion matrix, whose specific form can be found in **Appendix**;  $\mathbf{x}^{st} = [g_{g1}, g_{g2}, e_{ee}, e_{e3}, e_{le}, e_{13}, h_{1h}, h_{14}, h_{2h}, h_{24}, c_{3c}, h_{3h}, c_{4c}]$  represents the set of state variables of the EH, as indicated in Fig. 1;  $e^{in}$  and  $g^{in}$  are the electricity and gas consumptions, respectively;  $\rho^e$  and  $\rho^g$  are the nodal electricity and gas prices, respectively;  $(H_A, E_A), (H_B, E_B), (H_C, E_C), (H_D, E_D)$  are four combinations of heat and electric output of CHP, which serves as four extreme points to define a convex feasible operating region [7];  $ho_2^+$ ,  $ho_3^+$ ,  $co_3^+$ , and  $co_4^+$  are the heating/cooling capacities of GBL, EHP, and ACL, respectively;  $ho_2^-$ ,  $ho_3^-$ ,  $co_3^-$ , and  $co_4^-$  are the minimum heating/cooling outputs of these devices, respectively;  $el$ ,  $ht$ , and  $cl$  represent the energy types of electricity, heating, and cooling, respectively.

The optimal schedule in the day-ahead should be formulated for each EH in each hour. Denote the solutions for the  $n$ -th EH in the  $h$ -th hour as  $e^{in*}_{n,h}, g^{in*}_{n,h}, \mathbf{x}^{st*}_{n,h}$ .

#### B. Multi-Level Self-Scheduling of the EH in the Intraday

As shown in Fig. 3, the multi-level self-scheduling of the EH contains three strategies.

##### 1) First strategy: energy substitution

Energy substitution in the EH can reduce electricity consumption without load shedding, which has less interruption to users compared with traditional DR in the electricity system. The control variables of the energy substitution include the electricity consumption  $e^{in}$ , the gas consumption  $g^{in}$ , and the state variables  $\mathbf{x}^{st}$  of the EH. Apart from the same constraints (2)-(11) in the day-ahead scheduling, energy substitution should consider the DR capacity requirement:

$$e^{in}_{n,k} \leq e^{in*}_{n,h} - ER_{n,k}, k \in K \quad (12)$$

where  $ER_{n,k}$  is the requirement for DR capacity of the  $n$ -th EH at time period  $k$ ;  $K$  is the set of DR period, as marked in Fig. 2.

##### 2) Second strategy: temporal load shifting

The basic idea of the second strategy is to shift the energy

> REPLACE THIS LINE WITH YOUR MANUSCRIPT ID NUMBER (DOUBLE-CLICK HERE TO EDIT) <

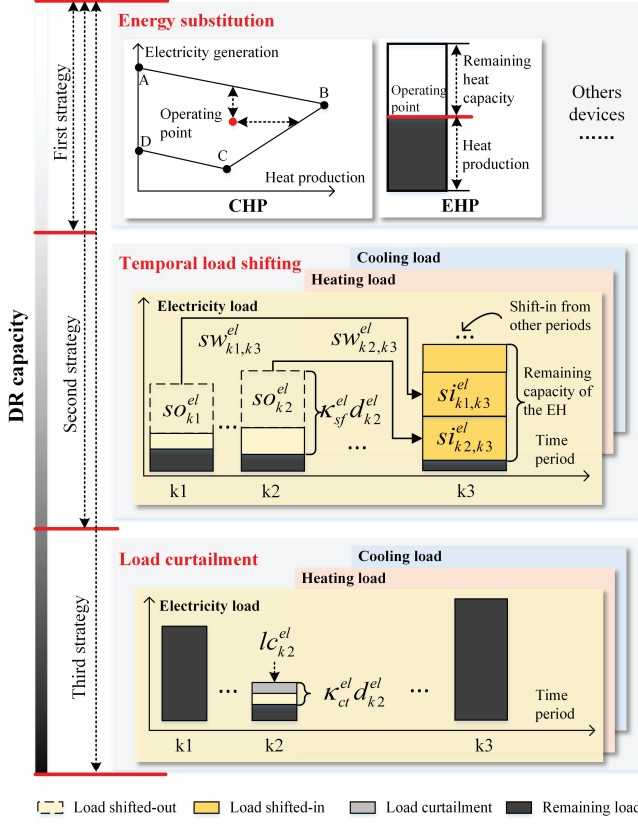


Fig. 3. Multi-level self-scheduling strategy of the EH.

loads among time periods to adjust the load profiles. For example, industrial users can rearrange the production plan, or residential users can reschedule their household appliances.

The temporal load shifting can be divided into two subprocesses, shift-out, and shift-in. The shift-out process is implemented in the electricity reduction period  $KD$ , as marked in Fig. 2. The available period for shifting-in  $KN$  ( $KN = K - KD$ ) should coincide with the users' preferences. For example, the shifted-out tasks (e.g., production plan) must be completed before the off-work time (e.g., 17:00). Then the latest time for shifting-in will be 17:00. Moreover, the duration for completing the tasks should be limited within  $SW_k^l$ . Thus, the whole temporal load shifting process can be described as:

$$\sum_{k' \in KN} sw_{k,k'}^l = SW_k^l, \forall k \in KD, sw_{k,k'}^l \in \{0,1\} \quad (13)$$

$$so_k^l = \sum_{k' \in KN} sw_{k,k'}^l \cdot si_{k,k'}^l, k \in KD \quad (14)$$

$$0 \leq si_{k,k'}^l \leq so_k^l \quad (15)$$

$$0 \leq so_k^l \leq \kappa_{sf}^l d_k^l \quad (16)$$

where  $sw_{k,k'}^l$  is a binary variable denoting whether the load of energy type  $l$  in period  $k$  is deployed to  $k'$ ;  $so_k^l$  is the quantity of the shifted-out load of energy type  $l$  in period  $k$ ;  $si_{k,k'}^l$  is the quantity of the energy load  $l$  shifted from period  $k$  to  $k'$ ;  $\kappa_{sf}^l$  is the maximum proportion of the shiftable load for energy type  $l$ .

The economic loss of temporary interruption by load shifting can be quantified using customer damage functions (CDF) [29].

Besides, the interruption cost is further related to the quantity of the shifted load, the energy type, and the interval between the shift-out and shift-in time. Therefore, the cost of the temporal load shifting can be calculated as:

$$C^{nd} = \sum_{k \in KD} \sum_{k' \in KN} \sum_{l \in \{el, ht, cl\}} sw_{k,k'}^l \cdot si_{k,k'}^l \cdot CDF^l(|k' - k|) \quad (17)$$

where  $CDF^l$  is the CDF for energy type  $l$ .

### 3) Third strategy: load curtailment

If the shifted-out load cannot be redeployed within the same day, the load curtailment will be implemented. The curtailed load of energy type  $l$  in period  $k$  is  $lc_k^l$ , which should be limited within a given boundary:

$$0 \leq lc_k^l \leq \kappa_{ct}^l d_k^l \quad (18)$$

where  $\kappa_{ct}^l$  is the maximum proportion of the curtailable load of energy type  $l$ . Moreover, CDF is also used to calculate the cost:

$$C^{rd} = \sum_{k \in KD} \sum_{l \in \{el, ht, cl\}} lc_k^l \cdot CDF^l \quad (19)$$

Summarizing all three strategies, we find that only the second strategy (i.e., temporal load shifting) is time-dependent. For example, if the load at the current time period  $k'$  is shifted into another period  $k$ , the load at the period  $k$  will be increased. Then, the original load  $d_k^l$  should be updated to load  $\tilde{d}_k^l$ :

$$\tilde{d}_k^l = \begin{cases} d_k^l - so_k^l - lc_k^l, & k \in KD \\ d_k^l + \sum_{k' \in KN} sw_{k,k'}^l \cdot si_{k,k'}^l, & k \in KN \end{cases} \quad (20)$$

which should also meet the constraints (2)-(11).

The formulation of the above self-scheduling strategy will be integrated into the optimization model in Section V. However, the bilinear terms in (14) will lead to an MINLP. Solving MINLP is extremely time-consuming and has no off-the-shelf reliable solvers. By using the McCormick envelope, we introduce an auxiliary variable  $\chi_{k,k'}^l = sw_{k,k'}^l \cdot si_{k,k'}^l$  to eliminate the bilinear terms [30]:

$$0 \leq \chi_{k,k'}^l \leq sw_{k,k'}^l \cdot \kappa_{sf}^l \cdot d_k^l \quad (21)$$

$$\chi_{k,k'}^l \leq si_{k,k'}^l \quad (22)$$

$$si_{k,k'}^l - \kappa_{sf}^l d_k^l (1 - sw_{k,k'}^l) \leq \chi_{k,k'}^l \leq \kappa_{sf}^l d_k^l \quad (23)$$

## IV. IEGS MODEL CONSIDERING LINEPACK FLEXIBILITIES

The self-scheduling strategy for EHs may lead to temporary spikes in the gas demands of IEGS. Unlike the electricity system that needs real-time balance, the spikes in gas demands can be covered by the gas stored in the transmission pipeline, which is also known as the linepack [17]. However, excessive abuse of linepacks could lower the pressure on adjacent gas buses and threaten the normal operation of the IEGS. To address this issue, this section first introduces the optimal day-ahead scheduling of IEGS to calculate the IEGS status, which can be further used to evaluate the available linepack. Then, the gas flow dynamics are modeled to ensure the security of IEGS after utilizing the linepack during the intraday DR.

### A. Optimal Scheduling of IEGS in the Day-Ahead

The optimal scheduling of the IEGS is implemented on an

> REPLACE THIS LINE WITH YOUR MANUSCRIPT ID NUMBER (DOUBLE-CLICK HERE TO EDIT) <

hourly basis. The objective is to minimize the operating cost:

$$\underset{w_i, g_{i,j}, g_{i,j}^{gfu}}{\text{Min}} \quad C^{\text{IEGS}} = \sum_{i \in GB} \rho_i^{\text{gs}} w_i + \sum_{i \in EB} \sum_{j \in NG_i} f_{i,j}^{\text{cst}}(g_{i,j}) \quad (24)$$

s.t.

$$w_i^- \leq w_i \leq w_i^+ \quad (25)$$

$$g_{i,j}^- \leq g_{i,j} \leq g_{i,j}^+ \quad (26)$$

$$g_{i,j}^{gfu,-} \leq g_{i,j}^{gfu} \leq g_{i,j}^{gfu,+} \quad (27)$$

$$w_i - q_i^d - \sum_{n \in EH_i} g_n^{in*} - \sum_{j \in NG_i^{gfu}} g_{i,j}^{gfu} / \zeta_{i,j} - \sum_{j \in \Omega_i^g} q_{ij} = 0 \quad (28)$$

$$\sum_{j \in NG_i^{gfu}} g_{i,j}^{gfu} + \sum_{j \in NG_i} g_{i,j} - e_i^d - \sum_{n \in EH_i} e_n^{in*} - \sum_{j \in \Omega_i^e} f_{ij} = 0 \quad (29)$$

$$q_{ij} = C_{ij} \text{sgn}(p_i - p_j) \sqrt{|p_i|^2 - |p_j|^2} \quad (30)$$

$$f_{ij} = (\theta_j - \theta_i) / X_{ij} \quad (31)$$

$$|f_{ij}| \leq f_{ij}^+ \quad (32)$$

$$|q_{ij}| \leq q_{ij}^+ \quad (33)$$

where  $C^{\text{IEGS}}$  is the operating cost of IEGS;  $\rho_i^{\text{gs}}$  is the gas purchasing price;  $w_i$  is the gas production at bus  $i$ ;  $g_{i,j}$  is the electricity generation of traditional fossil generating units (not gas-fueled)  $j$  at bus  $i$ ;  $f_{i,j}^{\text{cst}}$  is the generation cost function for traditional fossil generating units;  $EB$  and  $GB$  are the sets of electricity and gas buses, respectively;  $NG_i$  and  $NG_i^{gfu}$  are the sets of traditional fossil generating units and GFU at bus  $i$ , respectively;  $q_i^d$  and  $e_i^d$  are the gas and electricity demands excluding EHs, respectively;  $\zeta_{i,j}$  is the efficiency of the GFU;  $EH_i$  is the set of EHs at bus  $i$ ;  $\Omega_i^e$  and  $\Omega_i^g$  are the sets of electricity branches and gas pipelines connected to bus  $i$ , respectively;  $f_{ij}$  and  $q_{ij}$  are the electricity and gas flows from bus  $i$  to  $j$ , respectively;  $\theta$  is the phase angle;  $X_{ij}$  is the reactance of the branch;  $C_{ij}$  is a characteristic parameter of the pipeline, which depends on the length, absolute rugosity, and some other properties;  $\text{sgn}(x)$  is the signum function, where  $\text{sgn}(x)=1$  if  $x \geq 0$ , and  $\text{sgn}(x)=-1$  if  $x < 0$ .

Denote the solution of this problem at  $h$ -th hour as  $\mathbf{y}_h^{\text{st}*} = [w_{i,h}^*, g_{i,j,h}^*, g_{i,j,h}^{gfu*}]$ . Denote the solution of nodal gas pressure at bus  $i$  as  $p_i^*$ . Denote the nodal electricity and gas prices as  $\rho_i^{e*}$  and  $\rho_i^{g*}$  at bus  $i$ , respectively.

### B. Modelling of Gas Flow Dynamics for the Linepack Utilization in the Intraday

To ensure the security of linepack utilization during the DR, the gas flow dynamics are modeled. The gas flow dynamics in a pipeline are governed by two partial derivative equations (PDE), namely continuity and motion equations [31]:

$$\rho_0 B^2 A^{-1} \partial_x q + \partial_t p = 0 \quad (34)$$

$$\partial_x p + \rho_0 A^{-1} \partial_t q + 2\rho_0^2 B^2 (F^2 D A^2 p)^{-1} q |q| = 0 \quad (35)$$

where  $B$  is the isothermal wave speed of gas;  $\rho_0$  is the gas density at the standard temperature and pressure;  $A$  is the cross-sectional area of the pipeline;  $D$  is the diameter of the pipeline;  $F$  is the Fanning transmission factor.

The derivative regarding the time domain has little influence on the accuracy of (35), especially in the transmission pipelines with relatively steady flow rates and large capacities [32]. We

can discretize the above PDEs for the pipeline from bus  $i$  to  $j$  (the notation  $ij$  is omitted) using the Wendroff formula [31]:

$$B^{-2} (p_{m+1,k+1} + p_{m,k+1} - p_{m+1,k} - p_{m,k}) \quad (36)$$

$$+ \Delta t \rho_0 (\Delta x A)^{-1} (q_{m+1,k+1} - q_{m,k+1} + q_{m+1,k} - q_{m,k}) = 0$$

$$(p_{m+1,k+1} + p_{m+1,k})^2 - (p_{m,k+1} + p_{m,k})^2 + \Gamma \rho_0 B^2 (F^2 D A^2)^{-1} \Delta x (q_{m+1,k+1} + q_{m+1,k} + q_{m,k+1} + q_{m,k})^2 = 0 \quad (37)$$

where  $\Delta x$  and  $\Delta t$  are the step sizes in length and time domains, respectively;  $m$  is the index of pipeline segments;  $\Gamma = \text{sgn}(q_{ij}^*)$  represents the direction of the gas flow in the day-ahead.

Assume the gas flow does not change direction during the DR period [33]. Then, (37) can be further relaxed into SOC constraints:

$$\begin{cases} \left\| \begin{array}{l} p_{m,k+1} + p_{m,k}, \\ (\rho_0^2 B^2 (F^2 D A^2)^{-1} \Delta x)^{1/2} \\ (q_{m+1,k+1} + q_{m+1,k} + q_{m,k+1} + q_{m,k}) \end{array} \right\| \leq p_{m+1,k+1} + p_{m+1,k}, \Gamma = 1 \\ \left\| \begin{array}{l} p_{m+1,k+1} + p_{m+1,k}, \\ (\rho_0^2 B^2 (F^2 D A^2)^{-1} \Delta x)^{1/2} \\ (q_{m+1,k+1} + q_{m+1,k} + q_{m,k+1} + q_{m,k}) \end{array} \right\| \leq p_{m,k+1} + p_{m,k}, \Gamma = -1 \end{cases} \quad (38)$$

where penalty factor methods and sequential programming techniques can be used to drive the above relaxation tight [34].

Nodal gas pressure is the main factor that limits the utilization of linepack, which should be controlled within the secure limits during the DR period as (39). After formulating dynamic equations for all the pipelines, the initial conditions for those PDEs are specified as (40) and (41). For a set of connected pipelines, the boundary conditions are specified as (42) and (43):

$$p_i^- \leq p_i(x,t) \leq p_i^+ \quad (39)$$

$$p_{ij} \Big|_{t=0} = (p_i^{*2} - \text{sgn}(p_i^* - p_j^*) q_{ij}^{*2} (C_{ij}^2 L_{ij})^{-1} x)^{1/2} \quad (40)$$

$$q_{ij} \Big|_{t=0} = q_{ij}^* \quad (41)$$

$$\begin{cases} p_{ij} \Big|_{x=0} = p_{ij} \Big|_{x=L_{ij}} \quad (\forall j_1 \in \Omega_i^g) \\ p_{ij} \Big|_{x=0} = p_{j_2 i} \Big|_{x=L_{ij}} \quad (\forall j_2 \in \Omega_i^e) \end{cases} \quad (42)$$

$$w_{i,h}^* - q_i^d - \sum_{j \in NG_i^{gfu}} \frac{g_{i,j}^{gfu}}{\zeta_{i,j}} - \sum_{n \in EH_i} g_n^{in} + \sum_{j \in \Omega_i^e} q_{ji} \Big|_{x=L_{ji}} - \sum_{j \in \Omega_i^g} q_{ij} \Big|_{x=0} = 0 \quad (43)$$

where  $L_{ij}$  is the length of the pipeline from bus  $i$  to bus  $j$ .

## V. COORDINATED OPTIMAL CONTROL OF IEGS AND EHs

### A. Formulation of the Coordinated Optimal Control Problem

As shown in Sections III and IV, the operating conditions of EHs are tightly coupled with IEGS. Hence, a coordinated optimal control of IEGS and EHs is required. The objective is to minimize the total cost  $C^T$ :

$$\underset{\substack{p_{i,j,m,k}, q_{i,j,m,k}, g_{i,j,k}, \\ g_{i,j,k}^{gfu}, e_{i,j,k}^{in}, s_{i,j,k}^{in}, s_{i,j,k}^{rd}}}{\text{Min}} \quad C^T = C^E + \sum_{i \in EB} \sum_{n \in EH_i} (C_n^{nd} + C_n^{rd}) \quad (44)$$

&gt; REPLACE THIS LINE WITH YOUR MANUSCRIPT ID NUMBER (DOUBLE-CLICK HERE TO EDIT) &lt;

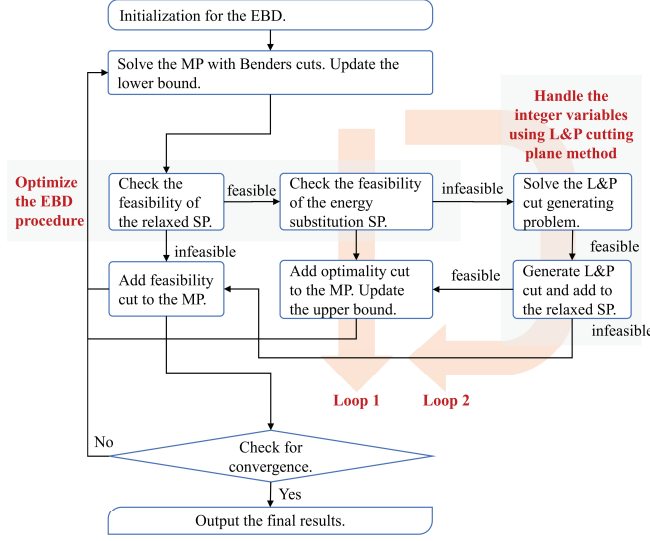


Fig. 4. Solution procedure of the EBD.

$$C^E = \sum_{k \in K} \left( \sum_{i \in EB} \left( \sum_{j \in NG_i} f_{i,j}^{ext}(g_{i,j,k}) + \rho_{i,k}^{g^*} \left( \sum_{n \in EH_i} g_{n,k}^{in} + \sum_{j \in NG_i^{gfu}} g_{i,j,k}^{gfu} / \xi_{i,j} \right) \right) \right) \quad (45)$$

where  $C^E$  is the energy cost;  $C_n^{nd}$  and  $C_n^{rd}$  are the costs of the temporal load shifting and load curtailment of  $n$ -th EH, respectively;  $\mathbf{x}_{n,k} = [\mathbf{x}_{n,k}^{st}, \mathbf{x}_{n,k}^{nd}, \mathbf{x}_{n,k}^{rd}]$  is the set of control variables of  $n$ -th EH in period  $k$ ;  $\mathbf{x}_{n,k}^{nd} = [so_{n,k}^l, si_{n,k,k'}^l, sw_{n,k,k'}^l, \chi'_{n,k,k'}]$ ,  $\forall k' \in KN$ ;  $\mathbf{x}_{n,k}^{rd} = lc_k^l$ . The optimization model is subject to:

- 1) *EH operating constraints*: (2)-(12). The load on the right-hand side of (2) should be replaced by the updated load  $\tilde{d}_k^l$ , as calculated in (20).
- 2) *EH self-scheduling constraints*: (13)-(23). Both EH operating and self-scheduling constraints should be formulated for all the EHs and all the time periods.
- 3) *IEGS operating constraints*: a) constraints for the gas system (36), (38)-(43), which should be formulated for all the pipelines at all the time periods; b) constraints for the electricity system (29), (31), and (32), which should also be formulated for all the periods; c) other trivial constraints (25), (26), and (33).

### B. Decentralized Solution Methodology

The IEGS and each EH generally belong to different entities and have their own regulations. To preserve their data privacies, these entities do not intend to share their system parameters. Therefore, a decentralized solution strategy based on Benders decomposition is proposed.

First, through reformulating the nonlinear constraints in the optimization models in (21)-(23) and (38), the original complex problem has been preliminarily simplified into a mixed-integer SOC programming problem. Then, considering the mathematical models of the IEGS and EHs are only linked via the electricity and gas consumptions, the decomposed structure is developed. The original optimization problem is decomposed

into an IEGS optimal control problem (i.e., the master problem (MP)) and several EH self-scheduling subproblems (SP). Due to the integer variables in the SPs, the Benders decomposition cannot be adopted straightforwardly. Therefore, we enhance it by embedding the lift-and-project (L&P) cutting plane method into the SPs, so that they can be convexified.

However, introducing the L&P cuts will increase the computation burden on solving the SPs. To address this issue, we improve the EBD procedure by further splitting the EH self-scheduling SP into two SPs: i) energy substitution SP; ii) load shifting-curtailing SP. The detailed solution procedure is presented in Fig. 4, which is also elaborated as follows:

#### 1) Initialization

Set the upper bound  $UB^{(0)}$ , lower bound  $LB^{(0)}$ , and tolerance  $\delta$  for the EBD.

#### 2) Solve the MP

$$\min_y \psi = C^E + \sum_{n \in EH} \psi_n \quad (46)$$

where  $\mathbf{y} = [p_{i,j,m,k}, q_{i,j,m,k}, g_{i,j,k}, g_{i,j,k}^{gfu}, e_{n,k}^{in}, g_{n,k}^{in}, \psi_n]$ . The MP subjects to (12), (26), (31), (32), (36), (38)-(43), and the Benders cuts from the SPs. The Benders cuts are initialized with  $\psi_n \geq 0$ , and are further supplemented by steps 4-6.

Denote the solution of MP in the  $s$ -th iteration as  $\hat{\mathbf{y}}^{(s)}$ , and the value of the objective function as  $\hat{\psi}^{(s)}$ . Update  $LB^{(s)} = \max\{LB^{(s-1)}, \hat{\psi}^{(s)}\}$ .

#### 3) Check the feasibility of the relaxed SP

The following relaxed SP for each EH is formulated and solved in parallel, given the solutions  $\hat{e}_{n,k}^{in,(s)}, \hat{g}_{n,k}^{in,(s)}$  from MP:

$$\min_{\mathbf{x}_{n,k}} \psi_n = C_n^{nd} + C_n^{rd} \quad (47)$$

which subjects to (2)-(23). The integer variables in (13) are relaxed into:

$$0 \leq sw_{k,k'}^l \leq 1, sw_{k,k'}^l \in \mathbb{R} \quad (48)$$

The relaxed SP is a linear programming problem, which can be easily checked for feasibility. If infeasible, go to step 4. Otherwise, obtain the solution  $\hat{\mathbf{x}}_{n,k}^{(s)}$ , and go to step 5.

#### 4) Add feasibility cut to the MP

Get the Farkas dual variables  $\lambda$  of each relaxed SP. Denote the constraints of the SP in a compact form:

$$\tilde{\mathbf{A}}^T [\mathbf{x}_n \mathbf{e}_n^{in} \mathbf{g}_n^{in}] \leq \mathbf{b} \quad (49)$$

where  $\tilde{\mathbf{A}} = [\mathbf{A} \mid \mathbf{A}_{e^{in}} \mathbf{A}_{g^{in}}]$ . Then, the following feasibility cut (44) is provided to the MP. Go to step 2 to start the next Benders iteration.

$$\lambda [\mathbf{A}_{e^{in}} \mathbf{A}_{g^{in}}]^T [\mathbf{e}_n^{in} \mathbf{g}_n^{in}]^T \leq \mathbf{b} \quad (50)$$

#### 5) Check the feasibility of the energy substitution SP

The energy substitution SP is formulated as:

$$\min_{\mathbf{x}_n^{st}} \{0 \mid s.t. (2)-(12)\} \quad (51)$$

The variables  $\mathbf{x}^{nd}$  and  $\mathbf{x}^{rd}$  are set to zero. If (51) is feasible, provide the optimality cut (52) to the MP, and go to step 1. Otherwise, go to step 6.

$$\psi_n \geq \lambda \mathbf{b} - \lambda [\mathbf{A}_{e^{in}} \mathbf{A}_{g^{in}}]^T [\mathbf{e}_n^{in} \mathbf{g}_n^{in}]^T \quad (52)$$

#### 6) Add L&P cut to the relaxed SP

For each integer variable  $sw_{k,k'}^l$ , if the solution  $\hat{sw}_{k,k'}^{l,(s)}$  in the relaxed SP is fractional, then formulate the following L&P cut

> REPLACE THIS LINE WITH YOUR MANUSCRIPT ID NUMBER (DOUBLE-CLICK HERE TO EDIT) <

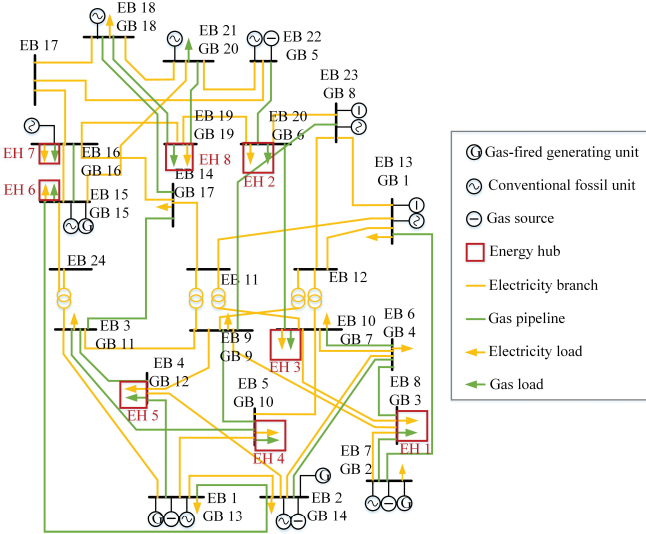


Fig. 5. Integrated electricity and gas test system with networked EHs.

generating problem [35]:

$$\min_{\alpha_{e^{in}}, \alpha_{g^{in}}, \alpha_x, \beta} \alpha_{e^{in}} \hat{e}_n^{in} + \alpha_{g^{in}} \hat{g}_n^{in} + \alpha_x \hat{x}_n - \beta \quad (53)$$

s.t.

$$\alpha = \mathbf{u}^T \tilde{\mathbf{A}} - u_0 \varepsilon_r \quad (54)$$

$$\alpha = \mathbf{v}^T \tilde{\mathbf{A}} + v_0 \varepsilon_r \quad (55)$$

$$\alpha = [\alpha_x \ \alpha_{e^{in}} \ \alpha_{g^{in}}]^T \quad (56)$$

$$\beta = \mathbf{u}^T b \quad (57)$$

$$\beta = \mathbf{v}^T b + v_0 \quad (58)$$

$$\mathbf{1}^T \mathbf{u} + \mathbf{1}^T \mathbf{v} + u_0 + v_0 = 1 \quad (59)$$

$$u, v, u_0, v_0 \geq 0 \quad (60)$$

where  $r$  is the order of this integer variable among all the variables;  $\varepsilon$  is the unit vector. The optimal solution  $\hat{\alpha}_{e^{in}}^{(s,r)}$ ,  $\hat{\alpha}_{g^{in}}^{(s,r)}$ ,  $\hat{\alpha}_x^{(s,r)}$ , and  $\hat{\beta}^{(s,r)}$  can be obtained by solving the problem (53)-(60).

The relaxed SP in step 3 can be then updated by supplementing the L&P cut (61):

$$\hat{\alpha}_{e^{in}}^{(s,r)} \hat{e}_n^{in} + \hat{\alpha}_{g^{in}}^{(s,r)} \hat{g}_n^{in} + \hat{\alpha}_x^{(s,r)} \mathbf{x}_n - \hat{\beta}^{(s,r)} \geq 0 \quad (61)$$

Solve the updated relaxed SP. If feasible, provide the optimality cut to the MP, similar to (52). Otherwise, add feasibility cut similar to (50). Then the upper bound can be updated as:

$$UB^{(s)} = \min \{UB^{(s-1)}, C^{E,(s)} + \sum_{n \in EH} \hat{\psi}_n^{(s)}\} \quad (62)$$

### 7) Convergence

Repeat the iteration from step 2 until the condition  $(UB - LB) / (UB + LB) < \delta$  is satisfied.

To sum up, the basic idea of the EBD procedure is that the load shifting-curtailing SP will only be checked, when both the relaxed SP is feasible and the energy substitution SP is infeasible. With this checking mechanism, the complex loop 2, as in Fig. 4, can be replaced by the simpler loop 1 for most of the scenarios. Therefore, the computation efficiency can be

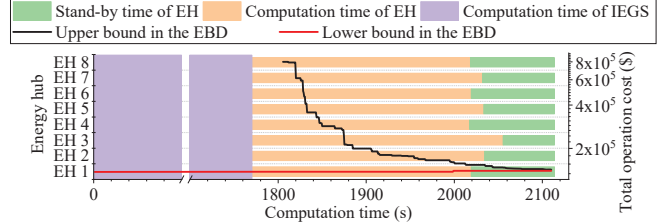


Fig. 6. Computation time of proposed solution strategy.

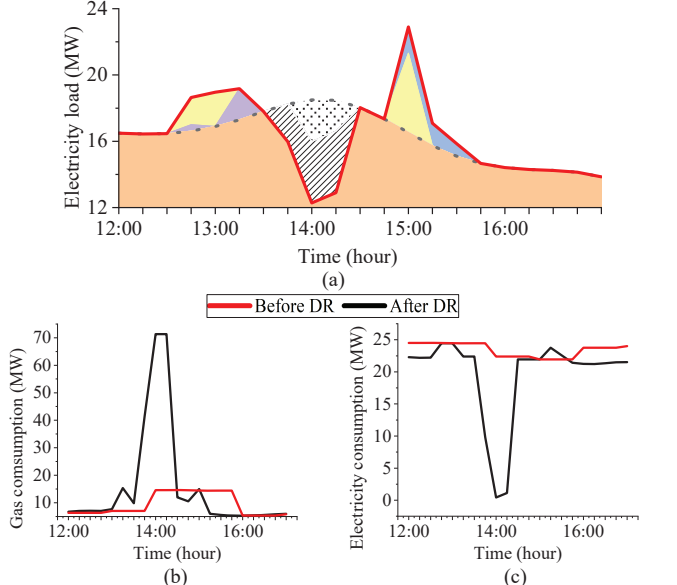
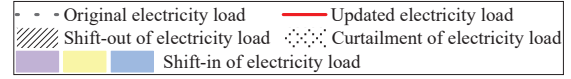
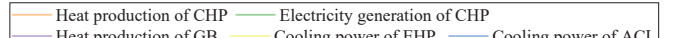


Fig. 7. (a) Shifting and curtailment of electricity load under a high stressed case. (b) Gas consumptions of the EH. (c) Electricity consumptions of the EH.

### Before the DR:



### During the DR:

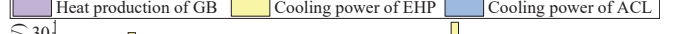
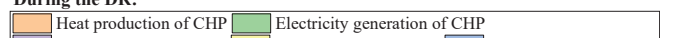


Fig. 8. Comparison of the operating conditions of EHs before and after DR. significantly improved.

## VI. CASE STUDIES

### A. Test System

In this section, an IEEE 24-bus Reliability Test System [36] and Belgium natural gas transmission system [37] are integrated to validate the proposed method. The two systems are topologically connected by GFUs and EHs, as presented in Fig. 5. The oil steam generating units with generation capacities of 12 MW, 20 MW, and 100 MW at electricity buses 15, 13, 14, and 2 are replaced by GFUs. The heat rate coefficients of GFUs and gas production prices of gas sources are set according to [38]. The configuration of EHs is the same as that in Fig. 1. It

> REPLACE THIS LINE WITH YOUR MANUSCRIPT ID NUMBER (DOUBLE-CLICK HERE TO EDIT) <

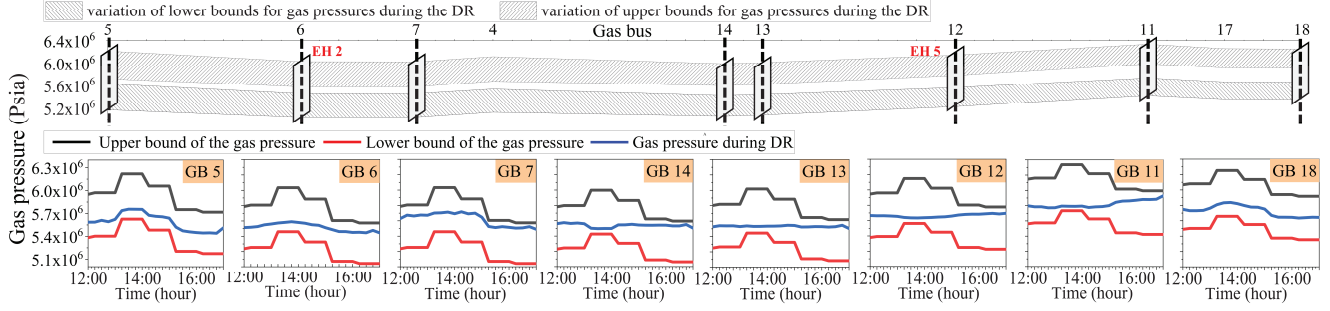


Fig. 9 Fluctuations of nodal gas pressures during DR.

Table 1. Operating condition of IEGS and EHs with different DR settings

Gas pressure fluctuation limit (%)	1.20%					1.30%	2.40%	0.50%
DR duration (h),	1.5	1.5	1.5	0.5	5	1.5	1.5	
DR capacity (%)	70%	40%	10%	70%	70%	70%	70%	
Total operating cost (\$)	$2.64 \times 10^5$	$2.60 \times 10^5$	$2.59 \times 10^5$	$2.60 \times 10^5$	$2.85 \times 10^5$	$2.51 \times 10^5$	$2.44 \times 10^5$	
Generation cost (\$)	$1.89 \times 10^5$	$1.91 \times 10^5$	$1.92 \times 10^5$	$1.91 \times 10^5$	$1.84 \times 10^5$	$1.91 \times 10^5$	$1.88 \times 10^5$	Infeasible
Gas purchasing cost (\$)	$7.43 \times 10^4$	$6.91 \times 10^4$	$6.63 \times 10^4$	$6.87 \times 10^5$	$1.00 \times 10^5$	$6.08 \times 10^4$	$5.39 \times 10^4$	
Load shifting/curtailment (MW)	25.97	8.02	0	0	40.99	8.97	0	

is assumed that half of the electricity load at peak hours is supplied by EHs. Based on that, the electricity, heating, and cooling loads, as well as the capacities of the devices in the EHs, are normalized according to [6]. The energy conversion efficiencies of the devices in the EHs are also set according to [6]. The proportions of the shiftable and curtailable loads are set to 20% and 10%, respectively [4].

The numerical simulations are performed on a laptop with an Intel® Core™ i7-8565U 1.80GHz and a 16GB memory. The optimization problems are solved using Gurobi. The self-scheduling SPs of EHs are parallelly processed by four cores.

#### B. Effectiveness of the Optimal Control for DR

To demonstrate the effectiveness of the optimal control for DR, a case with a large requirement for DR capacity is performed in this subsection. The peak value of the electricity load is increased by 0.3 times compared with the original Reliability Test System. The nodal gas pressures are limited to [0.95, 1.05] times of their values in the normal operating state. The DR signal is sent at 12:00. The DR period is set as 13:30-15:00. The available shifting-in period is set as 12:00-13:30 and 15:00-17:00. The DR capacity requirement is set based on the shortage of system reserve, e.g., 21.96 MW for EH 5.

The computation times are presented in Fig. 6. The total computation time is around 34 minutes, which is acceptable for the intraday operation. For most cases with fewer requirements for DR capacities, the problem can be solved within two minutes. The proposed solution method saves tremendous time, because most of the Benders cuts at the beginning are generated by solving the linear programming problem instead of the mixed-integer linear programming problem.

The electricity and gas consumptions of EH 5 before and after self-scheduling are compared in Fig. 7(b) and Fig. 7(c). During 13:30-14:30, the energy of electricity consumption reduced by DR is 60.34 MWh. The detailed self-scheduling process of the electricity load in EH 5 is explicated in Fig. 7(a). We can find that the load shifting and curtailment only account for 9.66 and 4.39 MWh, respectively. Most of the DR capacity is provided by energy substitution. The shifted-out electricity

loads are deployed to the adjacent periods, such as 12:45-13:15 and 15:00-15:45. These shift-in loads are well accommodated by the remaining capacities of the EH during these periods, without increasing the electricity consumption.

Fig. 8 shows the realization of the energy substitution from the perspective of specific devices in the EH. During the DR period 13:30-15:00, the outputs of electricity-consuming devices (e.g., EHP) are generally replaced by gas-consuming devices (e.g., CHP, GBL, and ACL). Therefore, the gas consumption of the EH increases significantly during 14:00-14:30, as presented in Fig. 7(b).

To observe the impact of gas demand spikes on the IEGS operation, the gas pressures along the critical pipeline route (e.g., the pipelines passing through GBs 5, 6, 7, 4, 14, 13, 12, 11, 17, and 18) are presented in Fig. 9. The variations of gas pressures at critical GBs along the route during the DR period are presented in detail. It can be seen that the gas pressures are controlled strictly and smoothly between the upper and lower bounds. For example, GB 6 is connected to EH 2. The EH's gas consumption increases dramatically during the DR. To deliver that, the gas source at upstream GB 5 ramps up its gas production to increase the linepack. The nodal pressure of GB 5 also increases to prepare for the DR. Therefore, the increased gas consumption during DR can be well accommodated by the coordinated optimal control of IEGS and EHs.

#### C. Comparisons of Various DR Requirements

Though the self-scheduling of EHs does not violate the IEGS security constraints, the fluctuation of gas pressure and utilization of linepack may still put the IEGS at a vulnerable state against future risks (e.g., load volatility or component failures). Therefore, key factors such as the DR capacity, operating cost, and gas pressure fluctuation limits should be balanced. For further investigation, the operating conditions of EHs and IEGS with various DR requirements, including DR capacities, DR durations, and gas pressure fluctuation limits are compared.

The simulation results are presented in TABLE I. In the

> REPLACE THIS LINE WITH YOUR MANUSCRIPT ID NUMBER (DOUBLE-CLICK HERE TO EDIT) <

$$\mathbf{H} = \begin{bmatrix} 0 & 0 & 1 & 0 & 0 & 1 & 0 & 0 & 0 & 0 & 0 & 0 & 0 & 0 & 0 \\ 0 & 0 & 0 & 0 & 0 & 0 & 0 & 0 & 1 & 1 & 0 & 0 & 1 & 0 & 0 \\ 0 & 0 & 0 & 0 & 0 & 0 & 0 & 0 & 0 & 0 & 0 & 0 & 0 & 1 & 1 \\ 1 & 0 & -1 & -1 & 0 & 0 & 0 & 0 & 0 & 0 & 0 & 0 & 0 & 0 & 0 \\ 0 & 1 & 0 & 0 & 0 & 0 & -1 & -1 & 0 & 0 & 0 & 0 & 0 & 0 & 0 \\ 0 & 0 & 0 & COP_3^h \gamma & COP_3^h \gamma & 0 & 0 & 0 & -1 & 0 & 0 & 0 & 0 & 0 & 0 \\ 0 & 0 & 0 & COP_3^c(1-\gamma) & COP_3^c(1-\gamma) & 0 & 0 & 0 & 0 & 0 & 0 & 0 & 0 & -1 & 0 \\ 0 & 0 & 0 & 0 & -1 & -1 & \eta_l^e & 0 & 0 & 0 & 0 & 0 & 0 & 0 & 0 \\ 0 & 0 & 0 & 0 & 0 & 0 & 0 & \eta_l^h & 0 & 0 & -1 & -1 & 0 & 0 & 0 \\ 0 & 0 & 0 & 0 & 0 & 0 & 0 & 0 & \eta_2 & 0 & 0 & 0 & -1 & -1 & 0 \\ 0 & 0 & 0 & 0 & 0 & 0 & 0 & 0 & 0 & 0 & 0 & COP_4 & COP_4 & 0 & 0 & -1 \end{bmatrix} \quad (63)$$

scenarios with the gas pressure fluctuation limits of 1.20%, the total operating cost, gas purchasing cost, and load shifting/curtailment are higher with the increase of the DR capacity and DR duration. By contrast, the generation cost is reduced, because the reserves are covered in part by the DR of EHs. With the relaxation of gas pressure limits from 1.20% to 1.30% and 2.40%, the EHs tend to have more flexibilities to perform self-scheduling, and thus the total operating cost and load shifting/curtailment can be reduced.

## VII. CONCLUSIONS

This paper proposes a coordinated optimal control framework of IEGS and EHs for providing DR services. A multi-level self-scheduling for the EH is developed by incorporating energy substitution, temporal load shifting, and load curtailment strategies. The gas flow dynamics of the linepack are utilized to accommodate gas demand spikes. To solve the optimal control problem, reformulation techniques are used to convexify both the load shifting and motion equations. The Benders decomposition is also enhanced with the L&P cutting plane method to solve this large-scale mixed-integer SOC programming problem in a decentralized manner. A unique solution procedure is further devised to reduce the computation burden.

The results verify that even under a highly stressed situation, the EHs can still demonstrate great potential for DR with the proposed method, which can achieve about 3 times of electricity reduction compared with that in traditional electricity DR. The fluctuation of nodal gas pressure can be also controlled within an appropriate range (e.g., 1.20%). This paper can assist the IEGS operators in devising the coordination strategies between the electricity and gas systems during the operational phase.

## APPENDIX: SPARSE ENERGY CONVERSION MATRIX

The specific formulation of the sparse energy conversion matrix is presented in (63), where  $COP_3^h$  and  $COP_3^c$  are the coefficients of performance of the EHP in heating and cooling mode, respectively;  $\gamma$  is the indicator for EHP operating mode, where  $\gamma=1$  represents heating mode, and  $\gamma=0$  represents cooling mode;  $\eta_l^e$  and  $\eta_l^h$  are the electrical and thermal efficiencies of the CHP, respectively;  $\eta_2$  is the thermal efficiency of the GBL;  $COP_4$  is the coefficient of performance of the ACL.

## REFERENCES

- [1] Y. K. Lei, K. Hou, Y. Wang, H. J. Jia, P. Zhang, Y. F. Mu, X. L. Jin, and B. Y. Sui, "A new reliability assessment approach for integrated energy systems: Using hierarchical decoupling optimization framework and impact-increment based state enumeration method," *Applied Energy*, vol. 210, pp. 1237-1250, Jan, 2018.
- [2] G. Xu, W. Yu, D. Griffith, N. Golmie, and P. Moulema, "Toward Integrating Distributed Energy Resources and Storage Devices in Smart Grid," *IEEE Internet of Things Journal*, vol. 4, no. 1, pp. 192-204, 2017.
- [3] M. Geidl, G. Koeppl, P. Favre-Perrod, and B. Klockl, "Energy hubs for the future," *IEEE Power & Energy Magazine*, vol. 5, no. 1, pp. 24-30, Jan-Feb, 2007.
- [4] S. Wang, C. Shao, Y. Ding, and J. Yan, "Operational reliability of multi-energy customers considering service-based self-scheduling," *Applied Energy*, vol. 254, pp. 113531, Nov, 2019.
- [5] C. Shao, Y. Ding, J. Wang, and Y. Song, "Modeling and Integration of Flexible Demand in Heat and Electricity Integrated Energy System," *IEEE Transactions on Sustainable Energy*, vol. 9, no. 1, pp. 361-370, Jul, 2018.
- [6] P. Mancarella, and G. Chicco, "Real-Time Demand Response From Energy Shifting in Distributed Multi-Generation," *IEEE Transactions on Smart Grid*, vol. 4, no. 4, pp. 1928-1938, Dec, 2013.
- [7] I. G. Moghaddam, M. Saniei, and E. Mashhour, "A comprehensive model for self-scheduling an energy hub to supply cooling, heating and electrical demands of a building," *Energy*, vol. 94, pp. 157-170, Jan, 2016.
- [8] M. Alipour, K. Zare, and M. Abapour, "MINLP probabilistic scheduling model for demand response programs integrated energy hubs," *IEEE Transactions on Industrial Informatics*, vol. 14, no. 1, pp. 79-88, Jul, 2018.
- [9] J. Ramos-Teodoro, F. Rodríguez, M. Berenguel, and J. L. Torres, "Heterogeneous resource management in energy hubs with self-consumption: Contributions and application example," *Applied Energy*, vol. 229, pp. 537-550, Nov, 2018.
- [10] T. Zhao, Y. Li, X. Pan, P. Wang, and J. Zhang, "Real-Time Optimal Energy and Reserve Management of Electric Vehicle Fast Charging Station: Hierarchical Game Approach," *IEEE Transactions on Smart Grid*, vol. 9, no. 5, pp. 5357-5370, Sep, 2018.
- [11] H. Hui, Y. Ding, W. Liu, Y. Lin, and Y. Song, "Operating reserve evaluation of aggregated air conditioners," *Applied Energy*, vol. 196, pp. 218-228, Jun, 2017.
- [12] S. Bahrami, and A. Sheikhi, "From Demand Response in Smart Grid Toward Integrated Demand Response in Smart Energy Hub," *IEEE Transactions on Smart Grid*, vol. 7, no. 2, pp. 650-658, Aug, 2016.
- [13] X. Zhang, M. Pipattanasompon, T. Chen, and S. Rahman, "An IoT-Based Thermal Model Learning Framework for Smart Buildings," *IEEE Internet of Things Journal*, vol. 7, no. 1, pp. 518-527, 2020.
- [14] T. Liu, D. Zhang, H. Dai, and T. Wu, "Intelligent Modeling and Optimization for Smart Energy Hub," *IEEE Transactions on Industrial Electronics*, vol. 66, no. 12, pp. 9898-9908, Dec, 2019.
- [15] B. Kazemi, A. Kavousi-Fard, M. Dabbaghjamanesh, and M. Karimi, "IoT-Enabled Operation of Multi Energy Hubs Considering Electric Vehicles and Demand Response," *IEEE Transactions on Intelligent Transportation Systems*, pp. 1-9, Jan, 2022.
- [16] Y. Gong, H. Yao, J. Wang, M. Li, and S. Guo, "Edge Intelligence-driven Joint Offloading and Resource Allocation for Future 6G Industrial Internet of Things," *IEEE Transactions on Network Science and Engineering*, pp. 1-1, 2022.

> REPLACE THIS LINE WITH YOUR MANUSCRIPT ID NUMBER (DOUBLE-CLICK HERE TO EDIT) <

- [17] S. Clegg, and P. Mancarella, "Integrated Electrical and Gas Network Flexibility Assessment in Low-Carbon Multi-Energy Systems," *IEEE Transactions on Sustainable Energy*, vol. 7, no. 2, pp. 718-731, Apr, 2016.
- [18] Z. Bao, D. Chen, L. Wu, and X. Guo, "Optimal inter- and intra-hour scheduling of islanded integrated-energy system considering linepack of gas pipelines," *Energy*, vol. 171, pp. 326-340, Mar, 2019.
- [19] L. Ni, W. Liu, F. Wen, Y. Xue, Z. Dong, Y. Zheng, and R. Zhang, "Optimal operation of electricity, natural gas and heat systems considering integrated demand responses and diversified storage devices," *Journal of Modern Power Systems and Clean Energy*, vol. 6, no. 3, pp. 423-437, May, 2018.
- [20] H. R. Massrur, T. Niknam, M. Fotuhi-Firuzabad, and A. Nikoobakht, "Hourly electricity and heat Demand Response in the OEF of the integrated electricity-heat-natural gas system," *IET Renewable Power Generation*, vol. 13, no. 15, pp. 2853-2863, 2019.
- [21] J. Yang, N. Zhang, C. Kang, and Q. Xia, "Effect of natural gas flow dynamics in robust generation scheduling under wind uncertainty," *IEEE Transactions on Power Systems*, vol. 33, no. 2, pp. 2087-2097, Mar, 2018.
- [22] N. Jia, C. Wang, Y. Li, N. Liu, and T. Bi, "Two-stage robust dispatch of multi-area integrated electric-gas systems: A decentralized approach," *CSEE Journal of Power and Energy Systems*, pp. 1-10, May, 2022.
- [23] H. Xie, X. Sun, C. Chen, Z. Bie, J. P. S. Catal, and x00E, "Resilience Metrics for Integrated Power and Natural Gas Systems," *IEEE Transactions on Smart Grid*, vol. 13, no. 3, pp. 2483-2486, May, 2022.
- [24] D. Huo, C. Gu, K. Ma, W. Wei, Y. Xiang, and S. L. Blond, "Chance-Constrained Optimization for Multienergy Hub Systems in a Smart City," *IEEE Transactions on Industrial Electronics*, vol. 66, no. 2, pp. 1402-1412, Aug, 2019.
- [25] W. Zhuang, S. Zhou, W. Gu, and X. Chen, "Optimized dispatching of city-scale integrated energy system considering the flexibilities of city gas gate station and line packing," *Applied Energy*, vol. 290, pp. 116689, May, 2021.
- [26] A. Bostan, M. S. Nazar, M. Shafie-khah, and J. P. S. Catalão, "Optimal scheduling of distribution systems considering multiple downward energy hubs and demand response programs," *Energy*, vol. 190, pp. 116349, Oct, 2020.
- [27] Y. He, M. Yan, M. Shahidehpour, Z. Li, C. Guo, L. Wu, and Y. Ding, "Decentralized Optimization of Multi-Area Electricity-Natural Gas Flows Based on Cone Reformulation," *IEEE Transactions on Power Systems*, vol. 33, no. 4, pp. 4531-4542, Dec, 2018.
- [28] C. Shao, Y. Ding, P. Siano, and Z. Lin, "A Framework for Incorporating Demand Response of Smart Buildings Into the Integrated Heat and Electricity Energy System," *IEEE Transactions on Industrial Electronics*, vol. 66, no. 2, pp. 1465-1475, Feb, 2019.
- [29] G. Wacker, and R. Billinton, "Customer cost of electric service interruptions," *Proceedings of the IEEE*, vol. 77, no. 6, pp. 919-930, Jun, 1989.
- [30] H. Zhou, Z. Li, J. H. Zheng, Q. H. Wu, and H. Zhang, "Robust Scheduling of Integrated Electricity and Heating System Hedging Heating Network Uncertainties," *IEEE Transactions on Smart Grid*, vol. 11, no. 2, pp. 1543-1555, Sep, 2020.
- [31] I. Cameron, "Using an excel-based model for steady-state and transient simulation," in PSIG Annual Meeting, St. Louis, Missouri, 1999, pp. 39.
- [32] A. Herrán-González, J. M. De La Cruz, B. De Andrés-Toro, and J. L. Risco-Martín, "Modeling and simulation of a gas distribution pipeline network," *Applied Mathematical Modelling*, vol. 33, no. 3, pp. 1584-1600, Mar, 2009.
- [33] Y. Zhou, C. Gu, H. Wu, and Y. Song, "An equivalent model of gas networks for dynamic analysis of gas-electricity systems," *IEEE Transactions on Power Systems*, vol. 32, no. 6, pp. 4255-4264, Nov, 2017.
- [34] Y. Li, Z. Li, F. Wen, and M. Shahidehpour, "Privacy-preserving optimal dispatch for an integrated power distribution and natural gas system in networked energy hubs," *IEEE Transactions on Sustainable Energy*, vol. 10, no. 4, pp. 2028-2038, Oct, 2019.
- [35] C. Li, and I. E. Grossmann, "A generalized Benders decomposition-based branch and cut algorithm for two-stage stochastic programs with nonconvex constraints and mixed-binary first and second stage variables," *Journal of Global Optimization*, vol. 75, no. 2, pp. 247-272, Oct, 2019.
- [36] C. Grigg, P. Wong, P. Albrecht, R. Allan, M. Bhavaraju, R. Billinton, Q. Chen, C. Fong, S. Haddad, S. Kuruganty, W. Li, R. Mukerji, D. Patton, N. Rau, D. Reppen, A. Schneider, M. Shahidehpour, and C. Singh, "The IEEE Reliability Test System-1996. A report prepared by the Reliability Test System Task Force of the Application of Probability Methods Subcommittee," *IEEE Transactions on Power Systems*, vol. 14, no. 3, pp. 1010-1020, Aug, 1999.
- [37] S. Wang, Y. Ding, C. Ye, C. Wan, and Y. Mo, "Reliability evaluation of integrated electricity-gas system utilizing network equivalent and integrated optimal power flow techniques," *Journal of Modern Power Systems and Clean Energy*, Oct, 2019.
- [38] C. Unsihuay, J. W. M. Lima, and A. C. Z. d. Souza, "Modeling the Integrated Natural Gas and Electricity Optimal Power Flow," in 2007 IEEE Power Engineering Society General Meeting, 2007, pp. 1-7.